Article

A Case Study of Open- and Closed-Loop Control of Hydrostatic Transmission with Proportional Valve Start-Up Process

Paweł Bury [1], Michał Stosiak [1,*], Kamil Urbanowicz [2], Apoloniusz Kodura [3], Michał Kubrak [3] and Agnieszka Malesińska [3]

[1] Department of Technical Systems Operation and Maintenance, Faculty of Mechanical Engineering, Wrocław University of Science and Technology, 50-371 Wrocław, Poland; pawel.bury@pwr.edu.pl

[2] Faculty of Mechanical Engineering and Mechatronics, West Pomeranian University of Technology in Szczecin, 70-310 Szczecin, Poland; kamil.urbanowicz@zut.edu.pl

[3] Faculty of Building Services, Hydro and Environmental Engineering, Warsaw University of Technology, 00-653 Warsaw, Poland; apoloniusz.kodura@pw.edu.pl (A.K.); michal.kubrak@pw.edu.pl (M.K.); agnieszka.malesinska@pw.edu.pl (A.M.)

* Correspondence: michal.stosiak@pwr.edu.pl

Abstract: This paper concerns the start-up process of a hydrostatic transmission with a fixed displacement pump, with particular emphasis on dynamic surplus pressure. A numerically controlled transmission using a proportional directional valve was analysed by simulation and experimental verification. The transmission is controlled by the throttle method, and the variable resistance is the throttling gap of the proportional spool valve. A mathematical description of the gear start-up process was obtained using a lumped-parameters model based on ordinary differential equations. The proportional spool valve was described using a modified model, which significantly improved the performance of the model in the closed-loop control process. After assuming the initial conditions and parameterization of the equation coefficients, a simulation of the transition start-up was performed in the MATLAB–Simulink environment. Simulations and experimental studies were carried out for control signals of various shapes and for various feedback from the hydraulic system. The pressure at the pump discharge port and the inlet port of the hydraulic motor, as well as the rotational speed of the hydraulic motor, were analysed in detail as functions of time. In the experimental verification, complete measuring lines for pressure, speed of the hydraulic motor, flow rate, and temperature of the working liquid were used.

Keywords: hydrostatic transmission; hydrostatic transmission start up; hydraulic drive

1. Introduction

In the case of heavy working machinery, some actuators often require low rotational speed values, ranging from a few to tens of rotations per minute. A crane rotation mechanism is an example of such equipment.

Hydrostatic drive units for low rotational speed movement can be constructed using two methods: with a high-speed hydraulic motor combined with an additional mechanical transmission, or with a low-speed motor coupled directly to the driven mechanism. In practice, however, a solution based on a hydrostatic transmission with a high-speed motor and mechanical transmission is used, as this is the only solution that can be applied in the case of a crane rotation mechanism [1]. This results from the need to comply with industry-specific legal regulations, which require using a mechanical brake to securely block the rotation mechanism in the event of external forces (wind, sloping ground within admissible limits, etc.). When a direct drive with a low-speed motor is used, the dimensions of the mechanical brake are quite large, particularly in the case of high load values.

The designer of the drive unit, apart from basic parameters, such as output power, speed range of the driven element, efficiency [2], etc., has to ensure specific dynamic

characteristics corresponding to the nature of the designed machinery [3]. In some cases, dynamic surplus is not allowed; for example, in the case of CNC machining tools, where the tool must be positioned right next to the machined surface without overshoot of the tool position.

Furthermore, the requirements applicable to machinery in dynamic states are constantly increasing. Modern machine and equipment evaluation criteria have recently been expanded to include vibration- and noise-level criteria, especially for hydrostatic drive machines [4]. Apart from their well-known advantages, hydrostatic drive units have a significant drawback—they generate relatively high noise emission levels, a factor which can disqualify this type of drive by causing them to exceed the standard noise emission levels (which are being gradually reduced), determined by ergonomic considerations [5–8]. It also means the necessity to reduce the risk of cavitation in hydrostatic systems [9] and the need for its proper modelling. However, limiting the maximum pressure during start-up will result in a reduction in the global noise emission level generated by the transmission in a transient state [10]. On the other hand, reducing the time during which the maximum pressure is generated will result in shortening of the time of the maximum noise levels of the unit during the start-up of the transmission. For a number of years, there has been an increasing tendency to reduce energy losses in mechanical systems, including hydraulic ones [11]. An increase in the efficiency of hydraulic systems can be achieved through control and adjustment of the hydraulic elements (valves, pumps, receivers), the use of systems featuring energy recuperation or hybrid systems, and reduction in dynamic loads [12]. Specific solutions make it possible to increase the efficiency of hydrostatic systems by several tens of percent. In the case of systems offering energy recuperation, the consumption of energy can be reduced by approx. 30% [13]. In hydrostatic systems, this can be achieved in a number of ways, depending on whether the system features fixed or variable displacement pumps. In systems with fixed displacement pumps controlled by throttle methods, the predominant approach is to limit the operation of the safety valve (where serial throttle control is used). The introduction of proportionally controlled valves (a proportional relief valve or a proportional spool valve) can also result in a reduction in energy consumption by the hydrostatic system, particularly in a transient state [14,15].

Additionally, dynamic surpluses (pressure and speed) occurring within the system contribute to excessive wear of the system elements and reduce the uptime [16].

Hydrostatic Transmission Control Methods

There are two basic methods for controlling a hydrostatic transmission in a hydrostatic drive unit: a throttle method and a volumetric method [17]. The throttle method involves an intentional modification of the flow resistance value (e.g., via an adjustable throttle valve) to regulate the value of the usable flow supply to the receiver. There are two types of control methods depending on the positioning of the adjustable throttle valve relative to the receiver—serial or parallel. In practice, the variable throttling gap is often obtained on the gaps of the spool–sleeve couple of the proportional spool valve. In the serial throttle control method, the use of a proportional valve for the purpose of throttling the usable flow supply to the receiver is justified by the fact that this solution enables changing the direction of the movement of the hydraulic receiver, among other factors. The continuous volumetric control method involves using a variable displacement pump and/or receiver.

This paper analyses a drive unit based on an M2C 1613 high-speed, hydraulic gear motor and an OH-500 three-stage planetary gear with a total gear ratio of $i = 69.7$. The paper investigates the impact of the parameters of the control signal for the proportional spool valve on the waveforms of the pressure and speed of the transmission, with a particular emphasis on the transient state during start-up. The transmission start-up process was examined according to the serial throttle control method. Additionally, a system featuring feedback from the speed of the hydrostatic motor and a PI numerical control system was analysed.

In the research on the control of hydraulic systems using proportional spool valve, many approaches can be found on how to model the opening characteristics of a hydraulic distributor. Very often, a linear or quadratic relationship between the spool displacement and the flow rate at a given differential pressure is adopted [18,19]. These methods often give satisfactory results for basic analysis of control systems that rarely operate at small valve openings. Unfortunately, when analysing closed-loop control systems, this approach can produce simulation results that differ significantly from experiment, which makes a proper machine control design process difficult.

Another method found in the literature is a very detailed modelling of the spool shape, which allows one to determine the cross-section of the orifice responsible for the flow [20]. This approach gives significantly better results than those of assuming a linear relationship; however, it does not take into account the phenomena associated with flow through a variable orifice. Additionally, such a spool modelling process requires one to obtain detailed documentation from the valve manufacturer, or the disassembly and detailed measurement of the spool and sleeve.

In this paper, a different method of spool modelling is presented, which does not require any additional documentation of the valve beyond the opening characteristic curve typically provided by the manufacturer.

It was assumed that the characteristic curve can be approximated with sufficient accuracy by a polynomial equation. A similar approach was presented by the authors of paper [21], but they did not present the implementation of this solution in the control system.

Figure 1 shows a diagram of a serial throttle control system for a hydrostatic transmission based on the use of a proportional valve, while Figure 2 shows schematics of the analysed control systems.
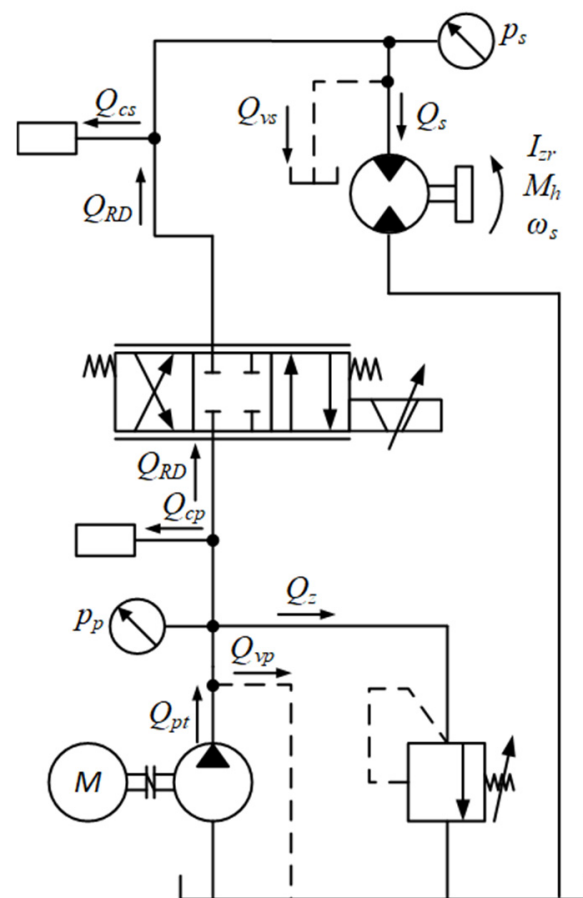
Figure 1. Diagram of the hydraulic system of a hydrostatic transmission with serial throttle control.

a)

b)
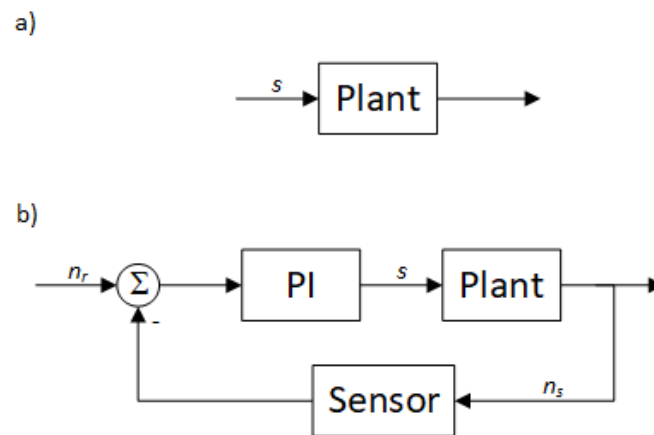
Figure 2. Diagrams of investigated control systems: (**a**) open-loop system; (**b**) closed-loop system.

2. Mathematical Model for the Serial Throttle Control Method

A mathematical description of the start-up of a hydrostatic transmission with serial throttle control using a proportional valve was obtained based on a set of ordinary differential equations (a model with focused parameters). One of the equations for the model is the flow continuity equation at particular points of the hydraulic circuit, and the other is the equation of the equilibrium of torque values on the shaft of the hydrostatic motor [22].

In order to solve this set of equations, it is also necessary to formulate the initial conditions.

In the presented mathematical model, the following simplifying conditions were adopted (among others):

- The temperature of the medium, and consequently its viscosity, remains constant throughout the simulation;
- The pressure has no effect on the viscosity of the medium;
- The compressibility of the medium and the deformability of the hydraulic elements was reduced to the concentrated capacitance at particular points of the system;
- There is no air in the system;
- There is no backlash in the mechanical system;
- The load of the motor is focused on its shaft (inertia);
- There are no wave phenomena;
- There are no external leaks in the system;
- The speed of the electric motor driving the pump is constant and is independent of the pump load;

The flow continuity equation can be formulated as follows:

$$Q_{pt} = Q_{vp} + Q_{cp} + Q_{RD} + Q_z \tag{1}$$

The throttling valve flow rate is determined as follows:

$$Q_{RD} = Q_s + Q_{vs} + Q_{cs} \tag{2}$$

$$Q_{RD} = G_{RD} \sqrt{p_p - p_s - p_d} \tag{3}$$

In a system with a proportional flow valve, it is usually assumed that there is a linear dependency between the area of the surface through which the liquid flows and the displacement of the spool. Unfortunately, this simplification does not work in simulations of systems where even the slightest displacement of the spool is a significant factor.

In the model, it was assumed that the aforementioned relation is a polynomial function (4), whose degree and values of coefficients were selected based on the characteristics

listed in the catalogue specification provided by the manufacturer of the spool valve. The result of model matching has been presented in Figure 3.

$$s_m = A_3 s^3 + A_2 s^2 + A_1 s + A_0 \tag{4}$$
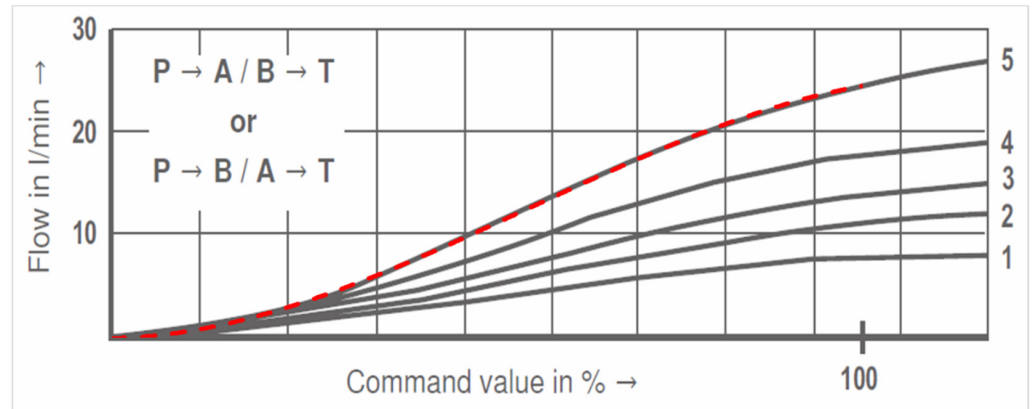
Figure 3. Opening characteristic curve of the spool valve from the data sheet with a fitted curve of model based on Equation (4). Curves 1–5 correspond to different valve pressure differential, the red dashed line is the fitted curve.

In the system with a proportional flow valve, it was assumed that the dynamics of the proportional flow valve are characterised by the following first-order differential equation, identical to the first-order inertial element:

$$s_m \cdot G_{RD\text{max}} = G_{RD} + T_{RD} \frac{dG_{RD}}{dt} \tag{5}$$

The flow through the hydraulic motor is described by the following equation:

$$Q_s = q_s \omega_s \tag{6}$$

The flow caused by the compressibility of the working medium [23] and the deformation of the elements of the system was assumed to be as follows:

- On the section from the pump to the proportional spool valve:

$$Q_{cp} = c_p \frac{dp_p}{dt} \tag{7}$$

- On the section from the proportional spool valve to the motor:

$$Q_{cs} = c_s \frac{dp_s}{dt} \tag{8}$$

Losses caused by leakages in the pump and in the motor can be described linearly with the following equations:

$$Q_{vp} = a_{vp} p_p \tag{9}$$

$$Q_{vs} = a_{vs} p_s \tag{10}$$

The pressure drop caused by the total loss of pressure resulting from viscous drag values (Hagen–Poiseuille equation) as well as the turbulent flow (Bernoulli's equation) were modelled using the following relation:

$$p_d = \frac{8\mu L Q_{RD}}{\pi R^4} + \sum_j \zeta_j \frac{\rho}{2} \left(\frac{Q_{RD}}{\pi R^2} \right)^2 \tag{11}$$

The equation of the flow through the safety valve can be presented in the following form [24]:

$$Q_z(t) = \begin{cases} h_z(p_p - p_0) - T_z\frac{dQ_z}{dt} & \text{for} \quad p_p > p_0 \\ 0 - T_z\frac{dQ_z}{dt} & \text{for} \quad p_p \le p_0 \end{cases} \tag{12}$$

In the analysed case, the motor load torque consists of three components: the constant one coming from static friction, the one coming from viscous friction in the motor and gearbox, and the moment of inertia. The torque value equilibrium condition on the hydrostatic motor shaft is described by the following relation:

$$q_s p_s = M_b + f\omega_s + I_{zr}\frac{d\omega_s}{dt} \tag{13}$$

To solve the above equations, the following initial conditions were assumed (slightly different from those found in the literature):

$$p_p(0) = p_0 + \frac{Q_{pt}}{h_z} \tag{14}$$

$$p_s(0) = 0 \tag{15}$$

$$Q_z(0) = Q_{pt} - a_{vp}p_0 \tag{16}$$

$$\omega_s(0) = 0 \tag{17}$$

The limit condition for the hydrostatic motor was defined as follows:

$$\text{if } q_s p_s \le M_b, \text{ then } \omega_s = 0, \frac{d\omega_s}{dt} = 0 \tag{18}$$

Solving the above equations numerically requires their parametrization; this was carried out based on the catalogue data and the information found in the literature. However, the available literature does not specify the value of some of the coefficients for the equations; therefore, experiments were conducted in order to determine the friction coefficient of the hydraulic motor and of the coupled planetary gear.

In hydrostatic drive units, damping is caused predominantly by internal leakage, resistance related to the flow of the working medium, and friction forces caused by the movement of the hydraulic motor and the driven mechanism. In the dynamic model of hydrostatic transmission, leakages are taken into account in the flow balance equation, while the resistance of the movement of the hydraulic motor and of the coupled mechanism (independent of the speed in the case of Coulomb friction and linearly dependent on the speed in the case of viscous friction) are described via the equation of the equilibrium of the torque values acting on the shaft of the motor. The viscous friction coefficients of the hydraulic motor and of the coupled planetary gear were determined by measuring the resistance to idle running motion as a function of the angular velocity of the shaft of the motor. The pressure differences, p_s, in the connection pipes of the hydraulic motor were taken as the measure of the aforesaid resistance values. Figure 4 shows the relation p_s as a function of the angular velocity, ω_s, of idle running. As the graph of this function shows, it is a linear relation, which—with accuracy sufficient for practical purposes—can be approximated with a straight line, which confirms the assumption of viscous friction.
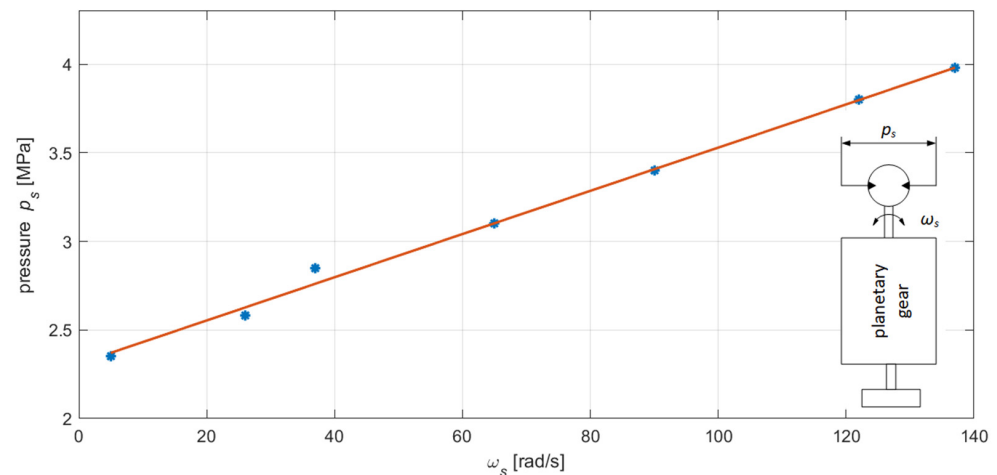
Figure 4. Resistance to motion of the gear motor M2C1613 and of the coupled planetary gear OH-500 as a function of angular velocity, ω_s, of idle running.

The findings presented here pertain to an M2C1613 gear motor coupled with an OH-500 planetary gear. The planetary gear was filled with SAE 85W90 transmission oil, whose temperature was kept within the range $t_1 = 25 - 28\,°C$ during the measurements, and the hydraulic motor was supplied with ISO-VG 46 hydraulic oil at a temperature of $t_2 = 40\,°C \pm 2\,°C$.

Based on the presented measurement results, one can determine the value of the viscous friction torque, and, in consequence, also the coefficient f of that friction, according to the following equation:

$$f = \frac{(p_s - p_c)q_s}{\omega_s} \tag{19}$$

Considering the specific absorptivity of the motor ($q_s = 5.03 \times 10^{-6}\,[\mathrm{m}^3\,/\mathrm{rad}]$), the viscous friction coefficient—determined based on the data presented in Figure 4, in accordance with Equation (19)—was $f = 6.3 \times 10^{-2}\,\left[\mathrm{N} \cdot \mathrm{m} \cdot \mathrm{s}/\mathrm{rad}^2\right]$.

Due to the specific nature of the rotational speed measurement, it was assumed in the model that the speed measurement system can be described using a first-order inertial element with the following transmittance:

$$G_n(s) = \frac{1}{T_n s + 1} \tag{20}$$

Once the equations of the mathematical model had been parametrized and the initial conditions adopted, it was possible to solve the model numerically, and subsequently to present in graphical form the pumping pressure of the pump, p_p, the pressure on the motor, p_s, and the angular velocity of the motor's shaft, n_s, over time, for various waveforms of the control signal, s, supplied to the coils of the proportional electromagnet, as described by Equation (21) and presented in graphical form in Figure 5:

$$s = \begin{cases} s_0 + \frac{s_{\max} - s_0}{t_0} t & \text{for } 0 < t < t_0 \\ s_{\max} & \text{for } t > t_0, \end{cases} \tag{21}$$
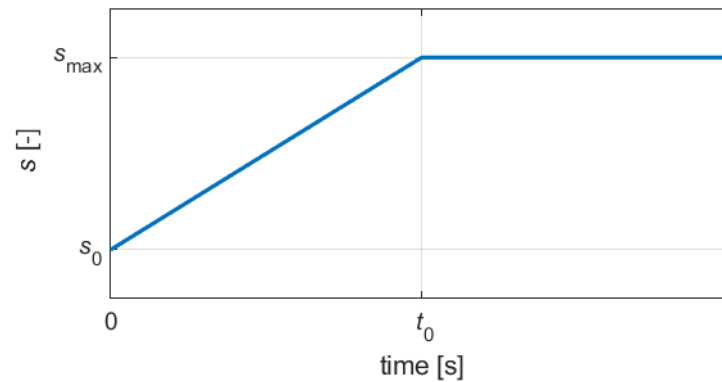
Figure 5. Waveform of the control signal, *s*, for the proportional valve.

The coefficient s_0 was taken in such a form as to compensate for the idle stroke of the spool of the proportional spool valve resulting from the stationary overlap, s_{max} was assumed to be the maximum value of the signal as specified in the specification sheet of the spool valve, and t_0 is the signal rise time from s_0 to s_{max}.

Figures 6–8 show the waveforms obtained by solving the mathematical models for, respectively, the pressure in the discharge flange of the pump p_p, the pressure at the inlet port of the motor p_s, and the rotational speed of the motor shaft n_s.
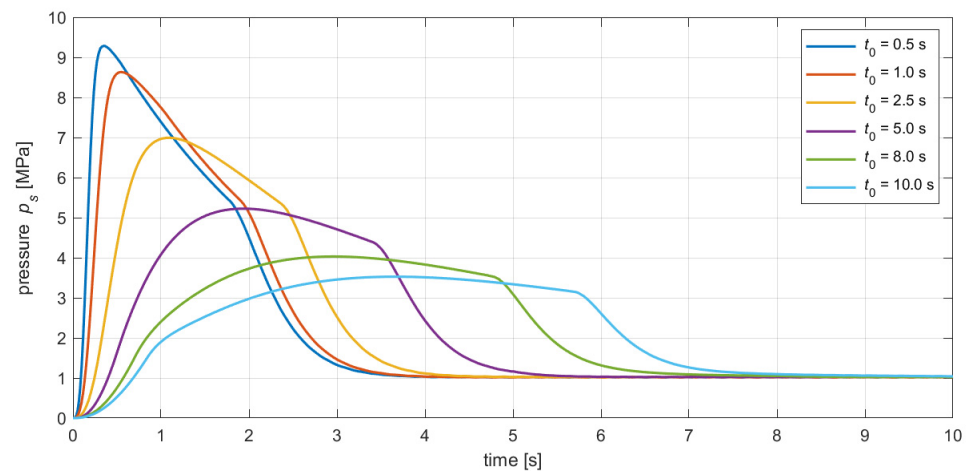
Figure 6. Result of simulation of the waveform of pressure on the motor p_s for various signal rise times, t_0.
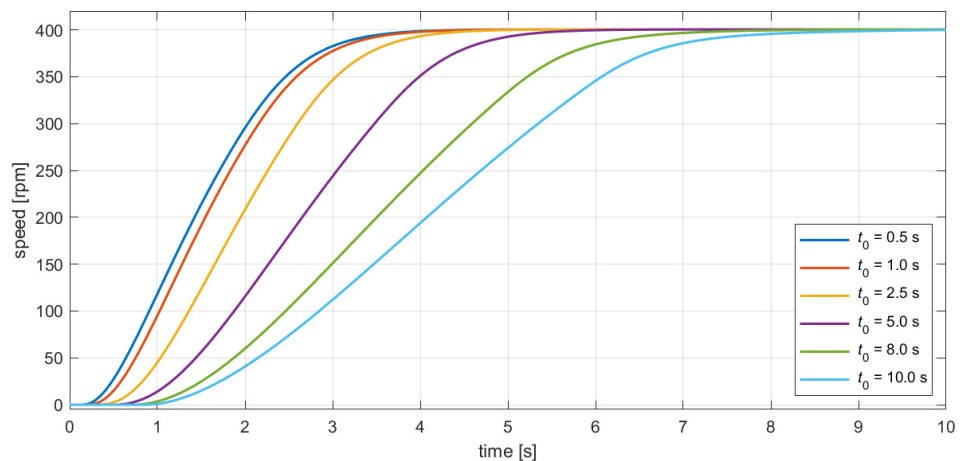
Figure 7. Result of simulation of the waveform of rotational speed n_s for various signal rise times, t_0.
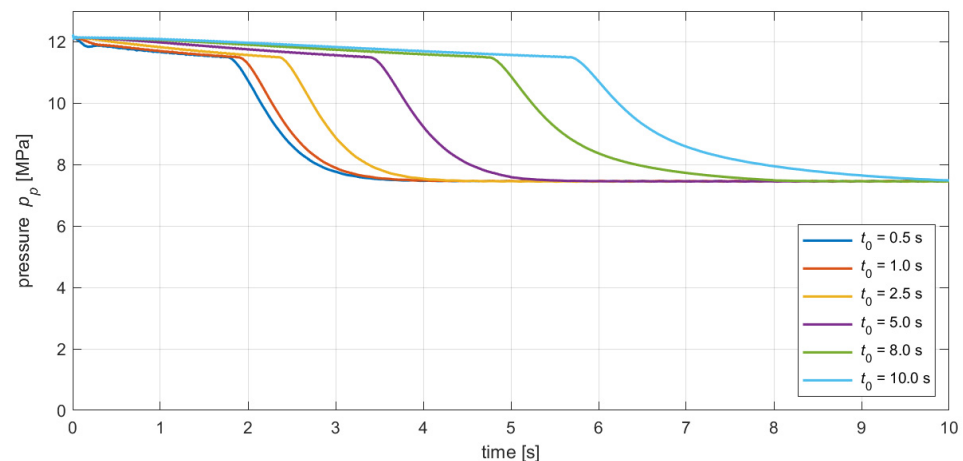
Figure 8. Result of simulation of the waveform of pressure on the pump p_p for various signal rise times, t_0.

The simulations were carried out for various values of the ramp time (edge rise time) $t_0 = \{ 0.5 \text{ s}, 1 \text{ s}, 2.5 \text{ s}, 5 \text{ s}, 8 \text{ s}, 10 \text{ s} \}$.

For the obtained results, the following parameters enabling assessment of the transitional state of the transmission were determined:

- Dynamic surplus pressure $p_{s \max}$ as the maximum pressure recorded during the start-up phase;
- Start-up time t_s as the time after which the rotational speed reaches 95% of the set value from the moment of supplying the control signal;
- Reaction time t_r as the time after which the speed of the motor reaches 5% of the set value;
- Energy E_s generated by the pump during the start-up process (first 10 s).

Table 1 presents a comparison of the parameters of the control signal along with the above-described values of the parameters for assessment of the transition state.

Table 1. Comparison of the control signal parameters and dynamic surplus pressure values at the inlet port of the motor, and the transmission start-up duration and reaction time. Transmission controlled with the serial throttle method without feedback.

t_0 [s]	$p_{s \max}$ [MPa]	t_s [s]	t_r [s]	E_s [Wh]
0.5	9.29	3.00	0.48	5.58
1.0	8.63	3.12	0.58	5.62
2.5	6.99	3.61	0.81	5.76
5.0	5.23	4.60	1.13	6.08
8.0	4.03	5.91	1.44	6.54
10	3.53	6.87	1.65	6.87

Analysing the simulation results obtained for the open control system (Figures 6–8 and Table 1), we can observe that for a signal rise time below $t_0 < 5$ s the start-up time, t_s, varies in a small range. This is directly due to the performance of the system, specifically the large moment of inertia and the maximum pressure set on the relief valve. Additionally, Table 1 shows the energy generated by the pump during start-up process. It can be observed that increasing the rise time of the signal increases the energy used for start-up. This is due to the fact that the pressure on the pump remains high for a longer period of time when the signal rise time is increased.

As the next step, the control system was equipped with a feedback loop from the angular velocity on the shaft of the hydraulic motor of the tested transmission. The following relation describes the transmittance of the PI controller used:

$$G_{PI}(s) = K_P \left(1 + \frac{1}{T_I s} \right) \tag{22}$$

The linear rise from $n_0 = 0$ rpm to the set value of $n_{max} = 200$ rpm was taken to be the signal of the set value to the controller, and $t_0 = 10$ s was taken to be the signal rise time. The following is the mathematical description of the signal of the set value:

$$n_r = \begin{cases} n_0 + \frac{n_{max} - n_0}{t_0} t & \text{for} \quad 0 < t < t_0 \\ n_{max} & \text{for} \quad t > t_0, \end{cases} \tag{23}$$

A series of simulations for various values of parameters of the PI controller was conducted for the assumed control signal. To assess the state of adjustment, apart from the above-mentioned parameters, two additional parameters were introduced:

- Overshoot parameter described by the following relation:

$$\kappa_n = \frac{\max\{n\}}{n_{max}} \tag{24}$$

- Steady-state error for the ramp input measured at the end of the ramp signal:

$$e_r = n_r - n_s \tag{25}$$

Table 2 presents a comparison of the parameters of the PI controller for which the simulation results are presented, as well as the determined values of the assessment parameters.

Table 2. Comparison of the parameters of the PI controller and the obtained values of the dynamic surplus pressure on the motor, the start-up time, the reaction time, and the overshoot.

K_P	T_I	$p_{s\,max}$ [MPa]	t_s [s]	t_r [s]	κ_n [%]	e_r [rpm]
0.020	0.50	2.70	9.72	1.49	102.7	4.4
0.020	0.75	2.34	9.84	1.63	101.8	6.4
0.020	1.00	2.15	9.94	1.73	100.9	8.8
0.015	0.50	2.51	9.79	1.70	102.7	5.7
0.015	0.75	2.19	9.94	1.87	101.6	8.6
0.015	1.00	2.03	10.09	2.00	100.5	11.5
0.010	0.50	2.28	9.93	2.05	102.6	8.5
0.010	0.75	2.04	10.16	2.28	101.2	12.9
0.010	1.00	1.91	10.39	2.45	-	17.4

The diagrams in Figures 9 and 10 illustrate the significant impact of the control and adjustment parameters on the waveforms of the pressure on the pump and on the motor, as well as the speed on the hydrostatic motor shaft.

Figures 11 and 12 show simulation results for different moments of inertia of the system in the range $I = 0.5 - 2.5 I_{zr}$. The presented model corresponds to other rotating systems of machines in which the moment of inertia changes significantly by changing the value and position of the load. In addition, the changes of the static load are insignificant, so it is assumed in the simulation that they are constant.
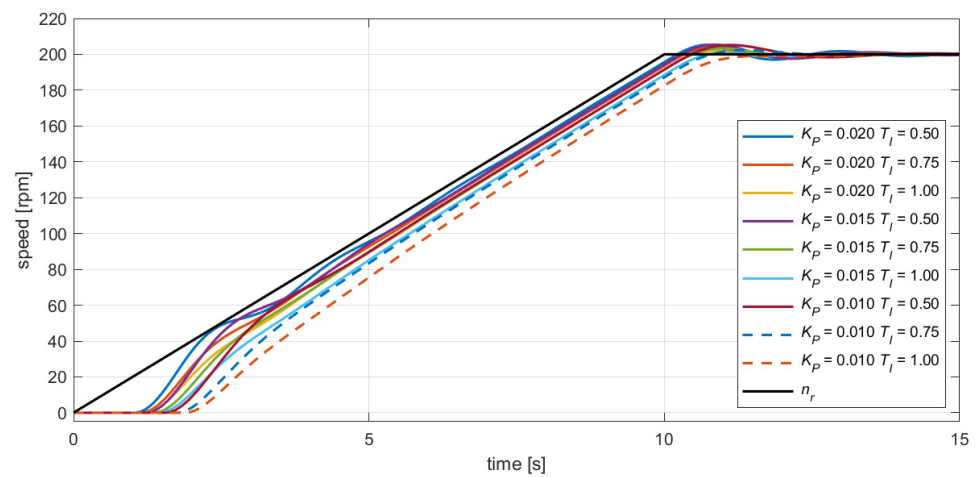
Figure 9. Result of simulation of the waveform of rotational speed, n_s, for various parameters of the PI controller.
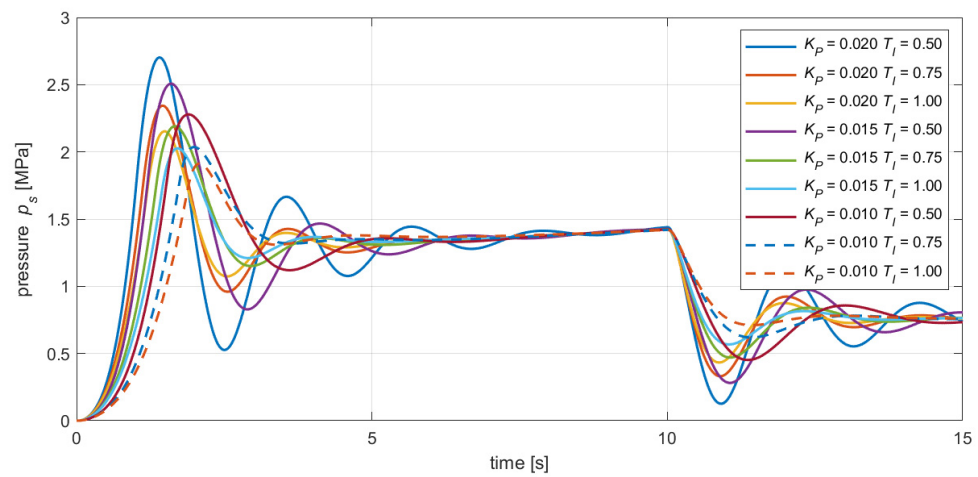
Figure 10. Result of simulation of the waveform of pressure on the motor p_s for various parameters of the PI controller.
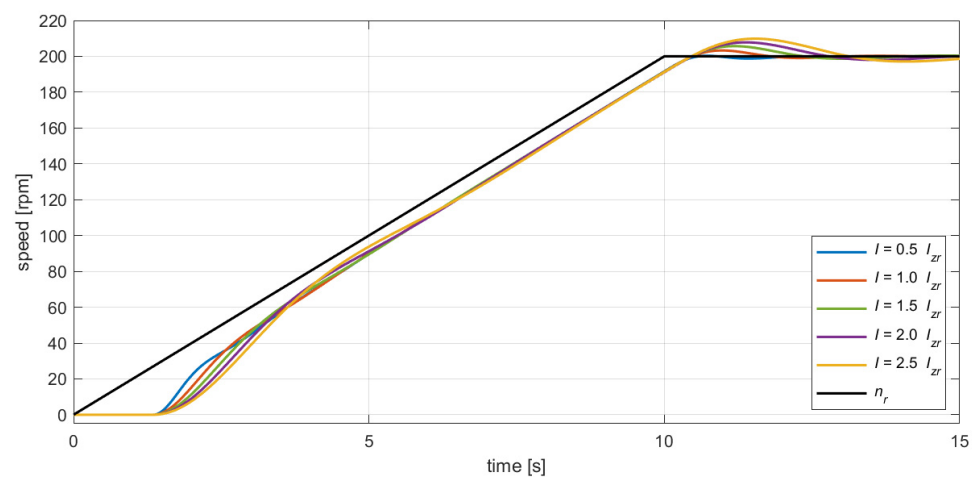
Figure 11. Result of simulation of the waveform of rotational speed, n_s, for various moments of inertia of the system ($K_P = 0.015$, $T_I = 0.75$ s).
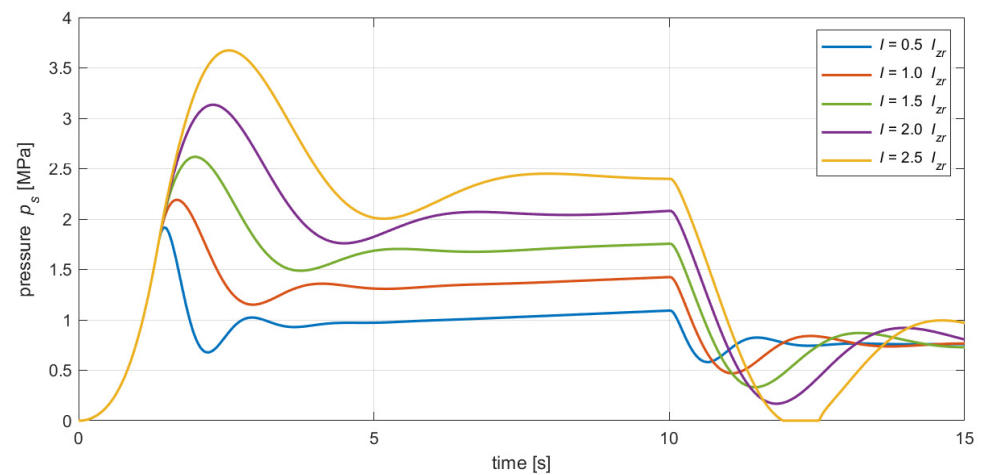
Figure 12. Result of simulation of the waveform of pressure on the motor p_s for various moments of inertia of the system ($K_P = 0.015$, $T_I = 0.75$ s).

3. Experimental Verification of the Mathematical Model

Experimental studies were conducted to verify the mathematical model, the assumed values of the parameters, and the assumptions. The experimental studies also made it possible to determine the relation between the shape (parameters) of the control signal for the proportional spool valve and the dynamic surplus pressure (at the inlet port of the motor) and the speed on the shaft of the motor. Additionally, the duration of the start-up process was analysed for various waveforms of the control signal for the proportional spool valve.

Figure 13 shows the test stand that was used to verify the model. The hydraulic power source is based on an axial variable displacement piston pump (flow was set to 14 L/min). The system is protected by a direct operating relief valve (nominal flow 25 L/min). A direct proportional spool valve (nominal flow 16 L/min) with spool position feedback was used to control the gear motor (size 32 cm^3/rev). The control signal was generated using a multifunction DAQ device with analogue I/O (NI USB-6001) connected to a PC with dedicated LabVIEW-based software. The measurement system was based on a 16-bit recorder (Hydrotechnik Multi System 8050) and piezoresistive pressure transducers (Hydrotechnik HySense PR100). The speed was measured using a tachometer (PZO E2/CPPB4).
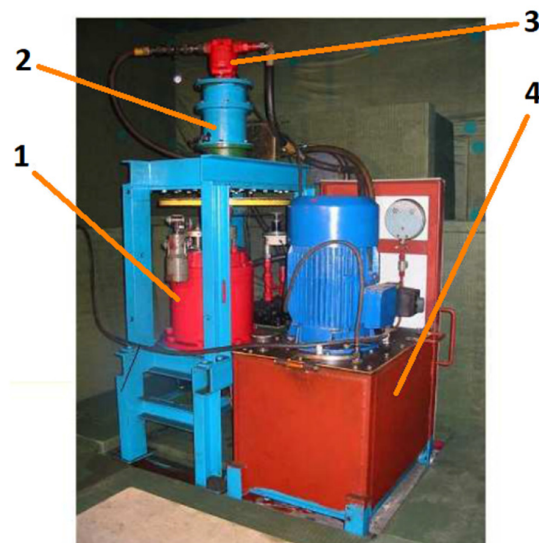
Figure 13. The hydrostatic transmission test stand: 1—planetary gear; 2—coupling housing; 3—hydraulic gear motor; 4—hydraulic power source.

Figures 14–16 show the waveforms obtained during the start-up of the transmission controlled by the serial throttle method with a proportional spool valve.
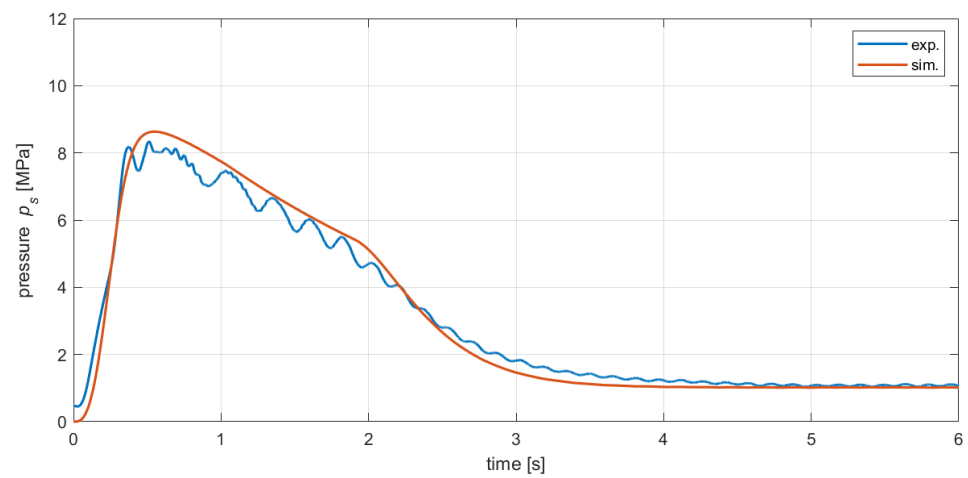
Figure 14. Measurement and result of simulation of the waveform of pressure on the motor p_s for the control signal rise time $t_0 = 1$ s.
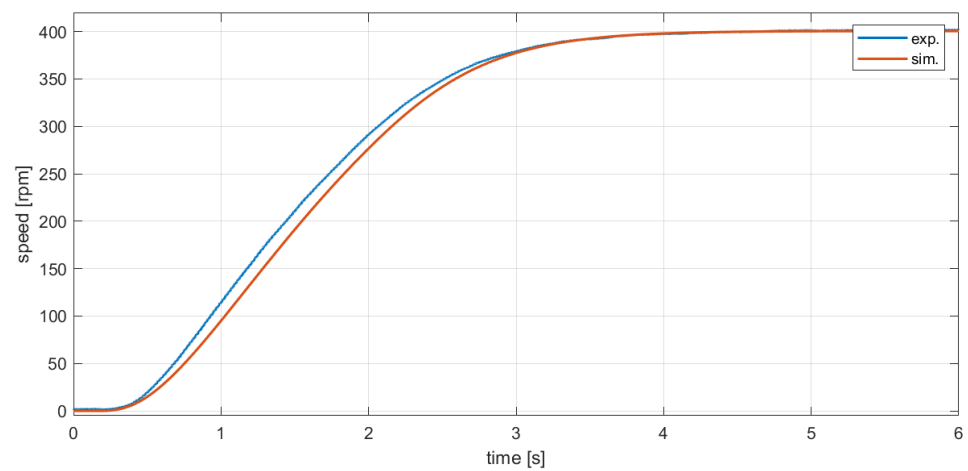
Figure 15. Measurement and result of simulation of the waveform of rotational speed on the motor, n_s, for the control signal rise time $t_0 = 1$ s.
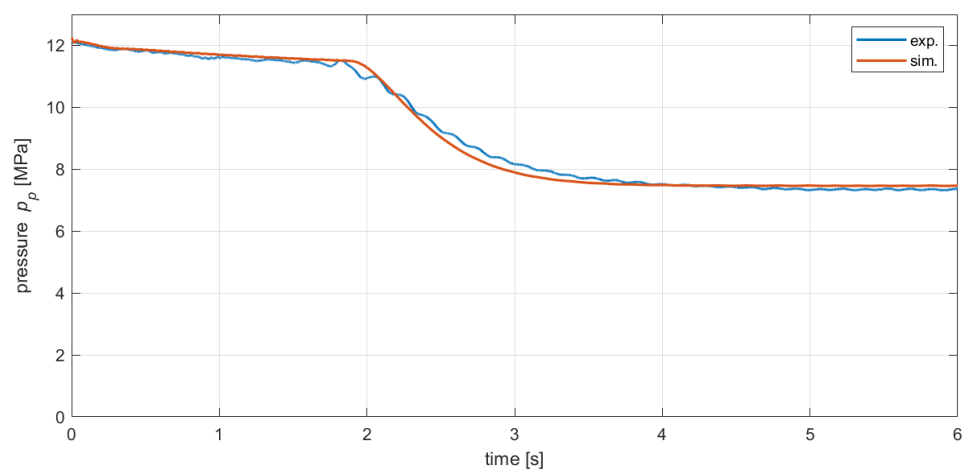
Figure 16. Measurement and result of simulation of the waveform of pressure on the pump p_p for the control signal rise time $t_0 = 1$ s.

In Figure 14, for the simulation time $t = 0$, the difference in pressure between the experiment and the result of simulation can be noticed. This difference is caused by the residual pressure remaining in the line from directional spool valve to the motor.

Figure 17 presents the result of two simulations compared with the experimental run. The simulation labelled "sim." is the result of the simulation including the opening characteristic fit (Equation (4)). In addition, the simulation labelled "sim.*" is shown, which assumes a linear dependence of flow on slider displacement ($s = s_m$), as in [18]. In the first control phase, a significant difference between the responses of different modelling approaches can be observed, which has a significant impact on the evaluation of the control dynamics.
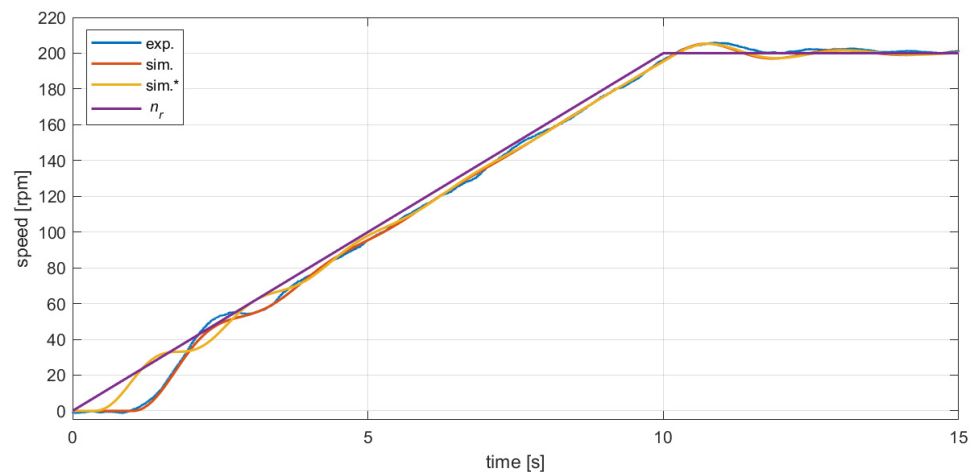
Figure 17. Measurement and result of simulation of the waveform of speed on the motor n_s for the control system ($K_P = 0.02$, $T_I = 0.5$ s). Waveforms labelled "sim." and "sim.*" shows the difference between simulation results with and without the modified spool valve model (Equation (4)).

The experimental verification studies demonstrate that the simulations satisfactorily model the actual transmission. This enables further work intended to optimise the parameters and the waveform of the control signal, which will result in a reduction in the dynamic surplus of the selected parameter (e.g., pressure at the inlet port of the motor) while maintaining control of the duration of the transitional process.

4. Conclusions

The paper describes the start-up process of a hydrostatic transmission controlled with a serial throttle. Additionally, it includes analyses of a transmission installed in a system equipped with a PI regulator controller. Based on the resulting waveforms over time, it can be concluded that during the start-up phase of an open-loop-controlled transmission with the serial throttle method, the positive-displacement pump operates under high load regardless of the ramp time of the proportional spool valve control signal. The pump high load time is correlated with the start-up time and the pressure waveform on the motor. However, the high load time of the pump can be reduced by suitably adjusting the parameters of the control signal supplied to the coils of the proportional spool valve. It was demonstrated that the maximum pressure value at the inlet port of the hydraulic motor during its start-up can be modified by adjusting the shape of the proportional spool valve control signal. In this way, it is also possible to reduce the noise generated by the transmission during start-up [25,26]. Therefore, reduction in the maximum pressure is an effective method for reducing the noise emission levels of a hydrostatic transmission in both transient and steady states. By adjusting start-up parameters (the control signal waveform), it is possible to regulate the maximum pressure value, the start-up time, and the reaction time. The start-up process can be also modified by selecting the shape of the spool of the proportional spool valve (e.g., symmetrical, asymmetrical) or by adjusting the stationary overlap and operational overlap, but these methods are not analysed in this paper. These

methods also result in reduction in the load of the elements of the transmission, which extends its operational life.

The method of modelling the hydraulic system presented in this paper, in particular the method of modelling the opening characteristics of the proportional spool valve, allows improving the simulation results obtained. The detailed construction of the model and conducting simulations enable initial adjustment and analysis of the control or regulation parameters prior to their application on the target machine. This is extremely important because it reduces the risk of errors during the prototype start-up phase, and therefore it reduces the time and costs of prototyping.

The presented detailed model for the start-up of the hydrostatic transmission equipped with a proportional valve can be used for the purpose of optimising the start-up process in terms of the execution of the objective function for the following parameters: dynamic surplus of a selected value, start-up time, reaction time, or the energy efficiency of the system.

Author Contributions: Conceptualization, M.S., P.B. and K.U.; methodology, M.S. and P.B; software, M.S. and P.B.; validation, M.S. and P.B.; formal analysis, M.S., P.B. and K.U.; investigation, M.S., P.B., A.K, M.K. and K.U.; resources, M.S. and P.B.; data curation, P.B.; writing—original draft preparation, M.S. and P.B; writing—review and editing, M.S., P.B., A.K., M.K. and A.M.; visualization, P.B., M.S. and A.M.; supervision, M.S. and P.B.; project administration, M.S.; funding acquisition, M.S. All authors have read and agreed to the published version of the manuscript.

Institutional Review Board Statement: Not applicable.

Informed Consent Statement: Not applicable.

Data Availability Statement: All coded generated during the study and experimental data are available from the corresponding author by request.

Nomenclature

a_{vp}	pump leakage coefficient $[\text{m}^3/\text{Pa·s}]$
a_{vs}	motor leakage coefficient $[\text{m}^3/\text{Pa·s}]$
A_0, A_1, A_2, A_3	coefficients of the polynomial function describing the opening of the spool valve $[-]$
c_p	capacitance of the liquid and of the pipes on the section from the pump to the proportional spool valve $[\text{m}^3/\text{Pa}]$
c_s	capacitance of the liquid and of the pipes on the section from the proportional spool valve to the motor $[\text{m}^3/\text{Pa}]$
e_r	steady-state error to ramp input $[\text{rpm}]$
E_s	energy generated by the pump during the first 10 s $[\text{Wh}]$
f	viscous friction coefficient $[\text{N·m·s}/\text{rad}^2]$
G_n	transmittance of the rotational speed measuring system
G_{PI}	PI controller transmittance
G_{RD}	conductivity of the spool valve $\left[\text{m}^3/\text{s}\sqrt{\text{Pa}}\right]$
$G_{RD\text{max}}$	maximum conductivity of the spool valve $\left[\text{m}^3/\text{s}\sqrt{\text{Pa}}\right]$
h_z	amplification factor of the relief valve $[\text{m}^3/\text{Pa · s}]$
i	gear ratio of the planetary gear $[-]$
j	summation index $[-]$
s_0	minimum value of the control signal $[-]$
s_{max}	maximum value of the control signal $[-]$
I_{zr}	reduced mass moment of inertia of rotational masses $[\text{kg · m}^2]$
K_P	proportional gain of the PI controller $[-]$
M_b	braking torque on the shaft of the hydrostatic motor $[\text{N·m}]$
L	total length of the pipes between the pump and the motor $[\text{m}]$

n	rotational speed of the hydrostatic motor [rpm]
n_0	initial rotational speed in the controlled system [rpm]
n_{max}	target rotational speed in the controlled system [rpm]
n_r	current rotational speed set point in the controlled system [rpm]
n_s	rotational speed on the shaft of the hydrostatic motor [rpm]
p_0	opening pressure of the relief valve [Pa]
p_d	total pressure drop resulting from flow rate losses [Pa]
p_p	pressure on the pump [Pa]
p_s	pressure on the hydraulic motor [Pa]
$p_{s\,max}$	dynamic surplus pressure on the motor [Pa]
p_c	pressure at the hydraulic motor corresponding to static resistance values (for $\omega \approx 0$) [Pa]
R	inner radius of the hydraulic pipes [m]
s	control signal [−]
s_m	modified control signal [−]
t	simulation time (step) [s]
t_0	control signal edge rise time [s]
t_1	oil temperature in the planetary gear [°C]
t_2	oil temperature in the hydraulic system [°C]
t_r	transmission reaction time [s]
t_s	transmission start-up time [s]
T_I	time constant of the integrating element of the PI controller [s]
T_n	time constant of the system for measuring the rotational speed [s]
T_{RD}	time constant of the spool valve [s]
T_Z	time constant of the relief valve [s]
q_s	displacement of the hydraulic motor [m^3/rad]
Q_{pt}	theoretical pump output flow [m^3/s]
Q_{vp}	flow value resulting from losses in the pump [m^3/s]
Q_Z	flow through the relief valve [m^3/s]
Q_{RD}	flow through the proportional valve [m^3/s]
Q_{cp}	flow caused by compressibility in volume between the pump and the spool valve [m^3/s]
Q_{cs}	flow caused by the compressibility in volume between the proportional spool valve and the hydraulic motor [m^3/s]
Q_s	flow towards the hydraulic motor [m^3/s]
Q_{vs}	flow value resulting from losses in the hydraulic motor [m^3/s]
ζ	coefficient of pressure losses caused by turbulent flow [−]
κ_n	speed overshoot in a PI controlled system [%]
μ	dynamic viscosity of the working medium [N · s/m^2]
ρ	density of the working medium [kg/m^3]
ω_s	angular velocity of the hydrostatic motor [rad/s]

References

1. Pullen, K.R.; Dhand, A. Mechanical and Electrical Flywheel Hybrid Technology to Store Energy in Vehicles. In *Alternative Fuels and Advanced Vehicle Technologies for Improved Environmental Performance*; Elsevier: Amsterdam, The Netherlands, 2014; pp. 476–504. ISBN 978-0-85709-522-0.
2. Comellas, M.; Pijuan, J.; Potau, X.; Noguès, M.; Roca, J. Efficiency sensitivity analysis of a hydrostatic transmission for an off-road multiple axle vehicle. *Int. J. Automot. Technol.* **2013**, *14*, 151–161. [CrossRef]
3. Xiong, S.; Wilfong, G.; Lumkes, J.J. Components Sizing and Performance Analysis of Hydro-Mechanical Power Split Transmission Applied to a Wheel Loader. *Energies* **2019**, *12*, 1613. [CrossRef]
4. Hubballi, B.; Sondur, V. Noise Control in Oil Hydraulic System. In Proceedings of the 2017 International Conference on Hydraulics and Pneumatics-HERVEX, Băile Govora, Romania, 8–10 November 2017.
5. Liu, J.; Yang, Y.; Suh, S. Hydraulic Fluid-Borne Noise Measurement and Simulation for Off-Highway Equipment. In Proceedings of the 2017 SAE/NOISE-CON Joint Conference (NoiseCon 2017), Grand Rapids, MI, USA, 11 June 2017.
6. Fiebig, W.; Wrobel, J. System Approach in Noise Reduction in Fluid Power Units. In Proceedings of the BATH/ASME 2018 Symposium on Fluid Power and Motion Control, Bath, UK, 12–14 September 2018; American Society of Mechanical Engineers: Bath, UK, 12 September 2018; p. V001T01A025.

7. Wróbel, J.; Blaut, J. Influence of Pressure Inside a Hydraulic Line on Its Natural Frequencies and Mode Shapes. In *Advances in Hydraulic and Pneumatic Drives and Control 2020*; Stryczek, J., Warzyńska, U., Eds.; Lecture Notes in Mechanical Engineering; Springer International Publishing: Cham, Switzerland, 2021; pp. 333–343. ISBN 978-3-030-59508-1.

8. Fiebig, W.; Wrobel, J.; Cependa, P. Transmission of Fluid Borne Noise in the Reservoir. In Proceedings of the BATH/ASME 2018 Symposium on Fluid Power and Motion Control, Bath, UK, 12–14 September 2018; American Society of Mechanical Engineers: Bath, UK, 12 September 2018; p. V001T01A026.

9. Zarzycki, Z.; Urbanowicz, K. Modelling of transient flow during water hammer considering cavitation in pressure pipes. *Inżynieria Chem. I Proces.* **2006**, *27*, 915–933.

10. Makaryants, G.M.; Prokofiev, A.B.; Shakhmatov, E. Vibroacoustics Analysis of Punching Machine Hydraulic Piping. *Procedia Eng.* **2015**, *106*, 17–26. [CrossRef]

11. Skorek, G. Study of Losses and Energy Efficiency of Hydrostatic Drives with Hydraulic Cylinder. *Pol. Marit. Res.* **2018**, *25*, 114–128. [CrossRef]

12. Karpenko, M.; Bogdevičius, M. Review of Energy-saving Technologies in Modern Hydraulic Drives. *Moksl.-Liet. Ateitis* **2017**, *9*, 553–558. [CrossRef]

13. Karpenko, M.; Bogdevičius, M. The Hydraulic Energy-Saving System Based on the Hydraulic Impact Effect. In Proceedings of the 10th National Conferences "Jūros ir krantų Tyrimai", Palanga, Lithuanian, 26–28 April 2017.

14. Lin, T.; Chen, Q.; Ren, H.; Miao, C.; Chen, Q.; Fu, S. Influence of the energy regeneration unit on pressure characteristics for a proportional relief valve. *Proc. Inst. Mech. Eng. Part I J. Syst. Control. Eng.* **2017**, *231*, 189–198. [CrossRef]

15. Domagała, Z.; Kędzia, K.; Stosiak, M. The use of innovative solutions improving selected energy or environmental indices of hydrostatic drives. *IOP Conf. Ser. Mater. Sci. Eng.* **2019**, *679*, 012016. [CrossRef]

16. Sobczyk, A.; Pobędza, J. Hydraulic Systems Safety by Reducing Operation and Maintenance Mistakes. *Syst. Saf. Hum.-Tech. Facil.-Environ.* **2019**, *1*, 700–707. [CrossRef]

17. Larsson, L.V. *Control of Hybrid Hydromechanical Transmissions*; Linköping Studies in Science and Technology; Division of Fluid and Mechatronic Systems, Department of Management and Engineering Linköping University: Linköping, Sweden, 2019.

18. Yao, Z.; Liang, X.; Zhao, Q.; Yao, J. Adaptive Disturbance Observer-Based Control of Hydraulic Systems with Asymptotic Stability. *Appl. Math. Model.* **2022**, *105*, 226–242. [CrossRef]

19. Acuna, W.; Canuto, E.; Malan, S. Embedded Model Control Applied to Mobile Hydraulic Systems. In Proceedings of the 18th Mediterranean Conference on Control and Automation, MED'10, Marrakech, Morocco, 23–25 June 2010; IEEE: Marrakech, Morocco, 2010; pp. 715–720.

20. Saleem, A.M.; Alyas, B.H.; Mahmood, A.G. Mathematical Model for a Proportional Control Valve of a Hydraulic System. *Int. J. Mech. Prod. Eng. Res. Dev. (IJMPERD)* **2020**, *10*, 8433–8444.

21. Tenesaca, J.; Carpio, M.; Saltarén, R.; Portilla, G. Experimental determination of the nonlinear model for a proportional hydraulic valve. In Proceedings of the 2017 IEEE International Autumn Meeting on Power, Electronics and Computing (ROPEC), Ixtapa, Mexico, 8–10 November 2017; pp. 1–4. [CrossRef]

22. Singh, R.B.; Kumar, R.; Das, J. Hydrostatic Transmission Systems in Heavy Machinery: Overview. *Int. J. Mech. Prod. Eng.* **2013**, *1*, 47–51.

23. Dasgupta, K.; Mandal, S.; Pan, S. Dynamic analysis of a low speed high torque hydrostatic drive using steady-state characteristics. *Mech. Mach. Theory* **2012**, *52*, 1–17. [CrossRef]

24. Morselli, S.; Gessi, S.; Marani, P.; Martelli, M.; De Hieronymis, C.M.R. Dynamics of pilot operated pressure relief valves subjected to fast hydraulic transient. *AIP Conf. Proc.* **2019**, *2191*, 020116. [CrossRef]

25. Chenxiao, N.; Xushe, Z. Study on Vibration and Noise for the Hydraulic System of Hydraulic Hoist. In Proceedings of the 1st International Conference on Mechanical Engineering and Material Science, Shanghai, China, 28–30 December 2012; Atlantis Press: Zhengzhou, China, 2012.

26. Stosiak, M. The impact of hydraulic systems on the human being and the environment. *J. Theor. Appl. Mech.* **2015**, *53*, 409–420. [CrossRef]